The Astrophysical Journal, 655: L65–L68, 2007 February 1

MID-INFRARED SPECTROSCOPY OF HIGH-REDSHIFT SUBMILLIMETER GALAXIES: FIRST RESULTS

Karín Menéndez-Delmestre,[1] Andrew W. Blain,[1] Dave M. Alexander,[2] Ian Smail,[2] Lee Armus,[3] Scott C. Chapman,[4,5] D. T. Frayer,[3] Rob J. Ivison,[6,7] and H. I. Teplitz[3]

Received 2006 October 30; accepted 2006 December 21; published 2007 January 12

ABSTRACT

We present mid-infrared spectra of five submillimeter galaxies at $z = 0.65$–2.38 taken with the *Spitzer Space Telescope*. Four of these sources, at $z \lesssim 1.5$, have strong PAH features and their composite spectrum is well fitted by an M82-like spectrum with an additional power-law component consistent with that expected from AGN activity. Based on comparison with local templates of the 7.7 μm PAH equivalent width and the PAH–to–infrared luminosity ratio, we conclude that these galaxies host both star formation and AGN activity, with star formation dominating the bolometric luminosity. The source at $z = 2.38$ displays a Mrk 231–type broad emission feature at rest frame $\sim$8 μm that does not conform to the typical 7.7 μm/8.6 μm PAH complex in starburst galaxies, suggesting a more substantial AGN contribution.

Subject headings: galaxies: active — galaxies: starburst — infrared: galaxies — techniques: spectroscopic

1. INTRODUCTION

Deep submillimeter-wave surveys (Smail et al. 1997; Barger et al. 1999; Eales et al. 1999; Cowie et al. 2002; Scott et al. 2002; Borys et al. 2003; Webb et al. 2003) have uncovered a population of ultraluminous infrared (IR) galaxies (ULIRGs; $L_{\rm IR} > (2\text{–}5) \times 10^{12}\ L_{\odot}$) at $z \sim 2$ (Blain et al. 2002). This observationally defined population of submillimeter galaxies (SMGs) coincides with the epoch of peak global star formation and quasar activity, with a significant contribution to the global star formation rate density at $z = 2$–3 not traced in the UV (Chapman et al. 2005, hereafter C05). Highly obscured by their dust content, the astrophysics of SMGs and the nature of their power source remain a challenge to address at optical and near-IR wavelengths (Chapman et al. 2003; C05; Swinbank et al. 2004). Deep X-ray studies suggest that $\sim$28%–50% of SMGs host an active galactic nucleus (AGN), although at face value it appears that the AGN does not dominate the bolometric luminosity and that powerful starbursts (SBs) contribute more significantly to the total energy output (Alexander et al. 2005, hereafter A05).

Less hindered by obscuration than shorter wavelengths, the mid-IR region boasts a number of spectral features, including: emission from polycyclic aromatic hydrocarbons (PAHs) (e.g., rest frame 6.2, 7.7, 8.6, 11.3, and 12.7 μm), associated with star formation (Helou 1999) and typically absent in powerful AGNs (Voit 1992); silicate absorption at 9.7 and 18 μm, which gives a measure of the obscuration by silicate dust grains along the line of sight to a small hot dust continuum source; and a hot dust continuum ($\lambda \lesssim 10$ μm), likely to be dominated by an AGN. The strength of these features have been used in mid-IR surveys with the *Infrared Space Observatory* (Genzel et al. 1998; Rigopoulou et al. 1999; Tran et al. 2001; Laurent et al. 2000) to estimate the relative contributions of SBs and AGNs for the brightest local galaxies (e.g., Rigopoulou et al. 1999). The spectra of the high-redshift population remained unexplored in the mid-IR until the advent of the *Spitzer Space Telescope* and the unprecedented sensitivity of the Infrared Spectrograph (IRS; Houck et al. 2004). Lutz et al. (2005, hereafter L05), Yan et al. (2005, hereafter Y05), Houck et al. (2005), Desai et al. (2006), and Weedman et al. (2006) have been among the pioneers in using IRS to study the mid-IR spectra of luminous sources at $z \sim 1$–3, extending to higher redshifts the analysis that was previously only accessible for nearby galaxies.

We have an IRS program to study the range of mid-IR properties of a sample of 24 high-z SMGs with $S_{24\,\mu{\rm m}} \gtrsim 0.4$ mJy, using the radio-identified sample with spectroscopic redshifts, compiled by C05. Here we present IRS spectra of the first five targets observed (SMM J221733+001120, SMM J163659+405728, SMM J030228+000654, SMM J163639+405636, and SMM J163650+405735): four are at lower redshift, with $z = 0.65$–1.5, and one is at $z = 2.38$. The low-redshift targets cover wavelengths longward of 10 μm and give insight into the longer mid-IR emission from SMGs; the full sample is more focused on $z \sim 2$ SMGs and hence probes shorter rest frame wavelengths. This preliminary sample is otherwise representative of the SMG population, in terms of bolometric luminosity, dust temperature, and submillimeter-to-radio flux ratio (C05).

2. OBSERVATIONS AND REDUCTION

We observed each target using the low-resolution Long-Low (LL) observing mode of IRS ($R \sim 57$–126) at two different nod positions for 30 cycles of 120 s each. We cover rest-frame emission longward of 6 μm to probe for PAH emission at 6.2, 7.7, 8.6, and 11.3 μm and for silicate absorption centered at 9.7 μm. The data were obtained between 2005 December and 2006 March.

The data were processed using the *Spitzer* IRS S13 pipeline,[8] which includes saturation flagging, dark subtraction, linearity correction, ramp correction, and flat-fielding. With a slit size of $\sim 10.5'' \times 168''$, IRS does not resolve the SMGs spatially, and the targets were treated as point sources throughout the data reduction and analysis. We performed additional reduction of the 2D spectra using IRSCLEAN[9] to remove rogue pixels, and relied on differencing between the nod positions to subtract

[1] California Institute of Technology, Pasadena, CA.
[2] Institute for Computational Cosmology, Durham University, Durham, UK.
[3] *Spitzer* Science Center, California Institute of Technology, Pasadena, CA.
[4] Institute of Astronomy, Cambridge, UK.
[5] CSA Fellow, University of Victoria, BC, Canada.
[6] UK Astronomy Technology Centre, Edinburgh, UK.
[7] Institute for Astronomy, Edinburgh, UK.

[8] See http://ssc.spitzer.caltech.edu/irs/dh.
[9] See http://ssc.spitzer.caltech.edu/archanaly/contributed/irsclean.

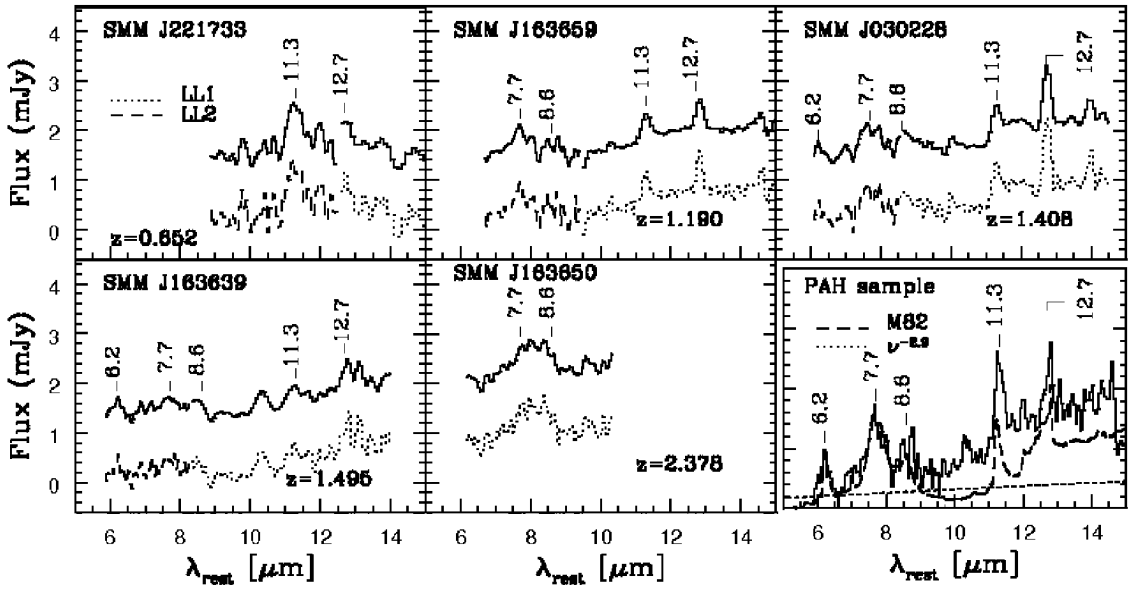

FIG. 1.—One-dimensional *Spitzer* IRS spectra for five SMGs and the composite spectrum of the PAH sample. For the five individual spectra, the lower curve represents the unsmoothed spectrum, with the first order (LL1: $\lambda_{obs} = 19.5$–38 μm) and second order (LL2: $\lambda_{obs} = 14$–21.3 μm) of the low-resolution mode shown in dotted and dashed lines, respectively. The upper curve shows the spectrum smoothed by 3 pixels and offset in flux for clarity. The various wavelengths of PAH emission features are indicated. We show the smoothed version of the composite spectrum for the PAH sample, together with the *ISO* SWS spectra of M82 (*dashed line*), smoothed to the resolution of IRS and normalized to the 7.7 μm PAH feature. The excess in the SMG composite, when fitted by M82, is consistent with an additional power-law component emission from an AGN (*dotted line*; see § 3.1.2).

the residual background. We used the *Spitzer* IRS Custom Extraction (SPICE)[10] software to optimally extract flux-calibrated 1D spectra, by taking a weighted average of profile-normalized flux at each wavelength to increase the S/N of these faint sources.

3. RESULTS AND DISCUSSION

The mid-IR spectra of SMM J221733, SMM J163659, SMM J030228, and SMM J163639 show moderate to strong PAH features (see Fig. 1), and we refer to these targets collectively as the "PAH sample." Detection of PAH emission is assumed to indicate the presence of SB activity. At most a very shallow dip is present around 9.7 μm in the spectra, indicating little silicate absorption.

Our highest redshift source, SMM J163650, is somewhat different from the other targets, with a broad feature at rest-frame ~8 μm, unlike the typical blended PAH complex of the 7.7 and 8.6 μm features found in SB galaxies. It is more reminiscent of the spectrum of Mrk 231 (Armus et al. 2007, hereafter A07), which features an unabsorbed continuum between absorption from silicates at longer wavelengths and hydrocarbons at shorter ones (Spoon et al. 2004, hereafter S04; Weedman et al. 2006). This similarity suggests that SMM J163650 has more substantial AGN activity than the SMGs in the PAH sample, as expected from the presence of a strong C IV (λ1549) feature at rest frame UV (C05) and a broad Hα component ($\simeq 1753 \pm 238$ km s^{-1}; Swinbank et al. 2004), both revealing the unambiguous presence of an AGN. We discuss the properties of this source in more detail in a subsequent paper discussing the full sample (K. Menéndez-Delmestre et al. 2007, in preparation) and concentrate here on the median properties of the SMGs with clear PAH emission.

To get an insight into the physics inherent to SMGs in our PAH sample, we compare their spectra with extensively studied local templates: the AGNs Mrk 231 (A07) and NGC 1068 (Sturm et al. 2000), the SB M82 (Förster Schreiber et al. 2003), and the ULIRGs Arp 220 (A07) and NGC 6240 (Armus et al. 2006, hereafter A06). Arp 220 has been a favorite template for high-redshift SMGs (Pope et al. 2006; Kovács et al. 2006): it has strong PAH features, indicative of SB activity, and a steep mid-IR continuum due to a heavily obscured nuclear component inferred to be responsible for the bulk of the IR luminosity (S04). AGNs have been identified in both merging components of NGC 6240, but SB activity dominates the total IR luminosity (Komossa et al. 2003).

A qualitative comparison of the spectra of our PAH sample with these templates rules out Mrk 231, NGC 1068, and Arp 220 as good matches, but the spectra are similar to those of M82 and NGC 6240. Similar results were found by L05, who detected strong PAH features in the spectra of two luminous SMGs at $z \sim 2.8$ that were well fitted by an M82-type spectrum.

3.1. *The Composite SMG Spectrum*

We take advantage of the similarity between the spectra in the PAH sample and of our precisely known redshifts (C05) to double our S/N, constructing a composite spectrum by averaging the individual spectra (Fig. 1). We use the composite spectrum to make a preliminary assessment of the independent contributions of SB and AGN activity in our PAH sample. Normalizing the local templates to the 7.7 μm peak in the composite spectrum, we find that the composite spectrum is well fitted at $\lambda \lesssim 9$ μm by the NGC 6240 and M82 spectra (Fig. 1). However, neither template provides a good fit to the composite spectrum at $\lambda \gtrsim 9$ μm: the continuum emission of NGC 6240 exceeds that of the composite spectrum at $\lambda \gtrsim 12$ μm, while the spectrum of M82 falls below it. No physically reasonable additional AGN component can be added to the NGC 6240 spectrum to produce a good fit to the com-

[10] See http://ssc.spitzer.caltech.edu/postbcd/spice.html.

posite spectrum at longer wavelengths. On the other hand, an M82-type spectrum plus a power-law continuum provides a good fit to the composite SMG data at all wavelengths.

3.1.1. *Starburst Component*

The 7.7 μm PAH feature is generally the most prominent in the mid-IR spectra of SB galaxies. Its strength relative to the continuum, measured by the equivalent width (EW), can be used to evaluate the fractional SB contribution to the total bolometric output, as the hot mid-IR continuum is enhanced significantly in the presence of an AGN. SB-dominated objects, such as M82 and NGC 6240, are characterized by larger PAH EWs than objects with a prominent AGN, such as Mrk 231.

EWs are sensitive to how the continuum is defined. We define a linear continuum by interpolating between two points clear of PAH emission, at 6.8 and 13.7 μm, or at 9 μm when the spectrum does not include one of these points. In Figure 2 we plot the 7.7 μm rest frame EWs and PAH-to-IR luminosity ratios for the SMGs in the PAH sample with 7.7 μm coverage and for the composite spectrum. The error in $L_{7.7\,\mu\mathrm{m}}/L_{\mathrm{IR}}$ for our SMG sample is dominated by a $\simeq$20% uncertainty in the IR luminosities (C05).[11] We compare a number of low- and high-redshift sources, including two ULIRGs at $z \sim 2$ with clear PAH detections from the Y05 sample with $S_{24\,\mu\mathrm{m}} \gtrsim 0.9$ mJy, and two SMGs (SMM J02399$-$0136 with $S_{850\,\mu\mathrm{m}} = 23$ mJy and MM J154127+6616 with $S_{850\,\mu\mathrm{m}} = 14.6$ mJy) at $z \simeq 2.8$ (L05).

According to the line-to-continuum (l/c) diagnostic presented by Genzel et al. (1998), systems with $(l/c)_{7.7\,\mu\mathrm{m}} \gtrsim 1$ are classified as SB$-$dominated and those with $(l/c)_{7.7\,\mu\mathrm{m}} < 1$, as AGN-dominated. With $(l/c)_{7.7\,\mu\mathrm{m}} \gtrsim 1$, SBs appear to dominate the Y05, L05, and our PAH sample.[12] However, the distribution in 7.7 μm EW and PAH–to–IR luminosity ratio in Figure 2 may suggest a distinction in the relative SB-to-AGN contributions, with lower values of these parameters indicating a stronger AGN contribution. We distinguish three regions in Figure 2: (1) a region with low PAH–to–IR luminosity ratios, occupied by Mrk 1014 (Armus et al. 2004) and the 24 μm–bright sample of Y05; (2) an intermediate PAH–to–IR luminosity region where NGC 6240 and the bulk of the SMGs in our sample are located; and (3) a region with the highest PAH–to–IR luminosity ratios, occupied by M82 and the two SMGs in L05.

At $z \sim 2$, 24 μm flux traces 8 μm rest-frame continuum; a stronger hot mid-IR continuum (produced by an AGN) dilutes the strength of PAH features, leading to lower $L_{7.7\,\mu\mathrm{m}}/L_{\mathrm{IR}}$. The location of the Y05 sample in the plot could follow from the selection of 24 μm–bright targets ($S_{24\,\mu\mathrm{m}} \gtrsim 0.9$ mJy) at this redshift, which would select objects with lower SB-to-AGN ratios. SMGs in our sample have higher $L_{7.7\,\mu\mathrm{m}}/L_{\mathrm{IR}}$ ratios, similar to NGC 6240, which we interpret as an indication of a markedly stronger SB contribution to the total luminosity than the Y05 sample. With similar IR luminosities, the location of the L05 SMG pair in this plot indicates that the 7.7 μm PAH feature is very strong. With large values for both the EW and the PAH–to–IR luminosity ratio, MM J154127 has been suggested as being dominated by SB activity (L05). The large PAH–to–IR luminosity ratio for SMG SMM J02399 suggests strong SB activity; however, the relatively low EW value, together with the evident strong mid-IR continuum (see Fig. 1 of L05), is consistent with this source having roughly equal AGN and SB contributions.

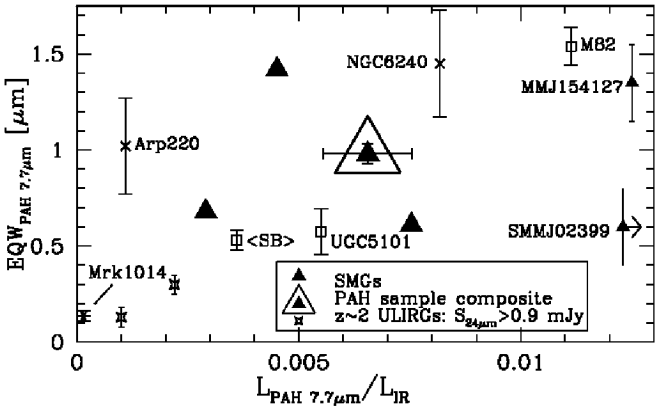

FIG. 2.—Relative strengths of the 7.7 μm PAH feature as measured by the PAH-to-IR (8–1000 μm) luminosity ratio and the rest-frame EW for the SMGs in the PAH sample (*large triangles*). We estimate the values for M82 (Förster Schreiber et al. 2003), Arp 220 (S04), NGC 6240 (A06) and the L05 pair of SMGs (*small triangles*) directly from their published spectra assuming a linear continuum slope; the error bars reflect the uncertainties of this approach. We derive a lower EW for NGC 6240 than A06, due to differences in continuum definition. Error bars for the Y05 sources, for the SB-dominated UGC 5101 (Armus et al. 2004), and for the average of 13 nearby SB galaxies studied with IRS (Brandl et al. 2006) reflect the uncertainties presented by the authors of the respective papers.

The SMGs in our PAH sample have values of $\mathrm{EW}_{7.7\,\mu\mathrm{m}}$ and $L_{7.7\,\mu\mathrm{m}}/L_{\mathrm{IR}}$ that place their SB-to-AGN ratio between that of the AGN-dominated ULIRG Mrk 1014 and the SB M82. This is qualitatively similar to NGC 6240, which has both SB and AGN components. As a caveat, we note that even though the 7.7 μm PAH–to–FIR luminosity ratio is associated to the SB-to-AGN ratio, it is also sensitive to details of the spectral energy distribution of the system, such as the presence of multiple dust components at different temperatures and the amount of extinction (e.g., Arp 220; S04). This may explain the particularly high 7.7 μm PAH–to–IR luminosity ratio for SMM J02399.

3.1.2. *The AGN Component*

Mid-IR line diagnostics suggest that SMGs are SB-like. The spectra of the SB-dominated galaxies M82 and NGC 6240 provide a good fit to the composite spectrum at $\lambda \lesssim 9$ μm; however, only an M82-type spectrum with an additional power-law AGN component gives a good fit to the composite spectrum at all wavelengths. The power-law component is defined as $S_\nu \sim \nu^{-2.9}$, consistent with the range of IR spectral indices for 3C quasars in Simpson & Rawlings (2000).

From the power-law component flux at 10.5 μm we estimate the X-ray luminosity (L_{X}) using the correlation between $S_{10.5\,\mu\mathrm{m}}$ and $S_{2-10\,\mathrm{keV}}$ presented by Krabbe et al. (2001). This yields $L_{\mathrm{X}} \sim 10^{44}$ ergs s^{-1} for an AGN at the average redshift for the SMGs presented in this paper, $z \sim 1.4$, in reasonable agreement with the X-ray luminosities found for the SMGs in A05. Following A05's approach, we compare the average X-ray–to–far-IR ratio of the SMGs in the PAH sample with the typical ratio for quasars and find that the residual flux is consistent with an underlying AGN contributing on the order of ~10% to the total far-IR emission. This agrees with the A05 result that AGN activity is often present in SMGs but does not dominate the energetics. Since the 10.5 μm excess is dominated

[11] Kovács et al. (2006) show that SMGs fall below the local FIR-radio relation and thus the C05-derived L_{IR} values, which rely on this relation, are on average overestimated by a factor of ~2.

[12] For our sample, $(l/c) \sim 1$ corresponds to EQW ~ 0.5 μm.

by lower redshift sources, further SMGs at $z \lesssim 2$, included in K. Menéndez-Delmestre et al. (2007, in preparation), will better constrain this excess.

4. CONCLUSIONS

We present first results of a *Spitzer* program to characterize the mid-IR spectra of high-redshift SMGs. We compare the spectra to well-studied local templates and find that SMGs have starburst mid-IR spectra more like M82 than the often quoted local analog Arp 220. The composite spectrum of the SMGs in the PAH sample is well fitted by an M82-like starburst component with a power-law continuum most likely representing a fainter underlying AGN. This similarity to the M82 spectrum suggests that the chemistry of the interstellar medium and radiation fields in these systems may be understood by looking at local galaxies in detail. Analysis of the 7.7 μm equivalent widths and PAH–to–IR luminosity ratios shows that SMGs are markedly different from the other 24 μm–selected samples, such as the ULIRGs at $z \sim 2$ (Y05), which have stronger AGN contributions. This work provides further evidence that SMGs host both star formation and AGN activity, but that star formation dominates the bolometric luminosity, reiterating the role of SMGs as the buildup sites for a significant fraction of the stellar content we see today.

An advantage of this sample is that by probing the lower redshift end of the C05 SMG sample distribution it provides rest-frame wavelength coverage longward of 9 μm to assess the AGN contribution. The SMG at $z = 2.38$, with a redshift closer to that of a typical C05 SMG, displays a potentially more AGN-dominated Mrk 231–type broad emission feature at rest frame $\sim$8 μm. The difference in AGN contributions within our preliminary sample suggests an increasing relative AGN activity in SMGs at higher redshifts, probably due to the 24 μm–based selection of targets. The full sample, with a more extended redshift distribution, will provide us with additional valuable information concerning the typical SMG population.

We thank our anonymous referee for valuable comments. We thank the *Spitzer* Science Center staff for their support, particularly Patrick Ogle for his help in the optimization of the spectral extraction. A. W. B. thanks the Research Corporation and the Alfred P. Sloan Foundation. D. M. A. and I. S. acknowledge support from the Royal Society. This work is based on observations made with the *Spitzer Space Telescope*, which is operated by the Jet Propulsion Laboratory, California Institute of Technology, under a contract with NASA. Support for this work was provided by NASA through an award issued by JPL/Caltech.

REFERENCES

Alexander, D. M., Bauer, F. E., Chapman, S., Smail, I., Blain, A., Brandt, W. N., & Ivison, R. 2005, ApJ, 632, 736 (A05)
Armus, L., et al. 2004, ApJS, 154, 178
———. 2006, ApJ, 640, 204 (A06)
———. 2007, ApJ, in press (astro-ph/0610218) (A07)
Barger, A. J., Cowie, L. L., & Sanders, D. B. 1999, ApJ, 518, L5
Blain, A., Smail, I., Ivison, R., Kneib, J.-P., & Frayer, D. T. 2002, Phys. Rep., 369, 111
Borys, C., Chapman, S., Halpern, M., & Scott, D. 2003, MNRAS, 344, 385
Brandl, B. R., et al. 2006, ApJ, 653, 1129
Chapman, S., Blain, A., Ivison, R., & Smail, I. 2003, Nature, 422, 695
Chapman, S., Blain, A., Smail, I., & Ivison, R. 2005, ApJ, 622, 772 (C05)
Cowie, L. L., Barger, A. J., & Kneib, J.-P. 2002, AJ, 123, 2197
Desai, V., et al. 2006, ApJ, 641, 133
Eales, S., Lilly, S., Gear, W., Dunne, L., Bond, J. R., Hammer, F., Le Fèvre, O., & Crampton, D. 1999, ApJ, 515, 518
Förster Schreiber, N. M., Sauvage, M., Charmandaris, V., Laurent, O., Gallais, P., Mirabel, I. F., & Vigroux, L. 2003, A&A, 399, 833
Genzel, R., et al. 1998, ApJ, 498, 579
Helou, G. 1999, in The Universe as Seen by *ISO*, ed. P. Cox & M. F. Kessler (ESA SP-427; Noordwijk: ESA), 797
Houck, J. R., et al. 2004, ApJS, 154, 18
———. 2005, ApJ, 622, L105
Komossa, S., Burwitz, V., Hasinger, G., Predehl, P., Kaastra, J. S., & Ikebe, Y. 2003, ApJ, 582, L15
Kovács, A., Chapman, S., Dowell, C. D., Blain, A., Ivison, R., Smail, I., & Phillips, T. G. 2006, ApJ, 650, 592
Krabbe, A., Böker, T., & Maiolino, R. 2001, ApJ, 557, 626
Laurent, O., Mirabel, I. F., Charmandaris, V., Gallais, P., Madden, S. C., Sauvage, M., Vigroux, L., & Cesarsky, C. 2000, A&A, 359, 887
Lutz, D., Valiante, E., Sturmn, E., Genzel, R., Tacconi, L., Lehnert, M., Sternberg, A., & Baker, A. 2005, ApJ, 625, L83 (L05)
Pope, A., et al. 2006, MNRAS, 370, 1185
Rigopoulou, D., Spoon, H. W. W., Genzel, R., Lutz, D., Moorwood, A. F. M., & Tran, Q. D. 1999, AJ, 118, 2625
Scott, S., et al. 2002, MNRAS, 331, 817
Simpson, C., & Rawlings, S. 2000, MNRAS, 317, 1023
Smail, I., Ivison, R., & Blain, A. 1997, ApJ, 490, L5
Spoon, H. W. W., Moorwood, A. F. M., Lutz, D., Tielens, A. G. G. M., Siebenmorgen, R., & Keane, J. V. 2004, A&A, 414, 873 (S04)
Sturm, E., Lutz, D., Tran, D., Feuchtgruber, H., Genzel, R., Kunze, D., Moorwood, A. F. M., & Thornley, M. D. 2000, A&A, 358, 481
Swinbank, A. M., Smail, I., Chapman, S., Blain, A., Ivison, R., & Keel, W. C. 2004, ApJ, 617, 64
Tran, Q. D., et al. 2001, ApJ, 552, 527
Voit, G. M. 1992, MNRAS, 258, 841
Webb, T. M. A., Lilly, S., Clements, D. L., Eales, S., Yun, M., Brodwin, M., Dunne, L., & Gear, W. 2003, ApJ, 597, 680
Weedman, D. W., Le Floc'h, E., Higdon, S. J. U., Higdon, J. L., & Houck, J. R. 2006, ApJ, 638, 613
Yan, L., et al. 2005, ApJ, 628, 604 (Y05)